

# The impact of the displacement of the both the tubular conductor and screen axes on the magnetic field in high current busducts

**Abstract.** In the paper it has been shown that as the distance  $d$  between the axis of the tubular conductor increases the magnetic field becomes more and more non-uniform. The phenomenon of the inducing of eddy currents in the screen makes the magnetic field distribution changed in the screen itself and its surroundings. The magnitude of these changes depends on  $\lambda$  and  $\alpha$  coefficients, thus the screen electrical conductivity and its transverse dimensions, the current frequency in the phase conductor, and the mutual geometrical configuration between the tubular conductor and screen.

**Streszczenie.** W artykule pokazano, że w miarę wzrostu odległości  $d$  między osiami przewodów, pole magnetyczne staje się coraz bardziej nierównomiernie. Zjawisko indukowania prądów wirowych w ekranie zmienia rozkład pola magnetycznego w nim samym i jego otoczeniu. Wielkość tych zmian zależy od współczynników  $\lambda$  oraz  $\alpha$ , a więc od konduktywności ekranu i jego wymiarów poprzecznych, częstotliwości prądu w przewodzie fazowym oraz wzajemnej konfiguracji geometrycznej między tym przewodem a ekranem. (**Wpływ przesunięcia osi przewodu i ekranu na pole magnetyczne w torach wielkoprądowych.**)

**Key words:** magnetic field, tubular screen, high current busduct

**Słowa kluczowe:** pole magnetyczne, ekran rurowy, tor wielkoprądowy

## Introduction

In high current busducts one or more phase tubular conductors are isolated with a tube screen. The magnetic field of the conductor (conductors) induces eddy currents in the shield which generate a reverse reaction magnetic field. The resultant magnetic field within the internal and external area of the shield is the vector sum of these fields. In the general case of two concentric tubular conductors the axes of the conductors do not coincide, and create the so-called non-coaxial system (fig.1) [1,2].

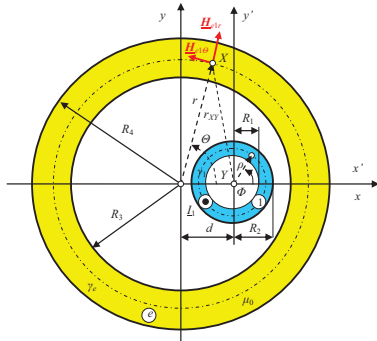


Fig. 1. Tubular screen with the internal non-coaxial tubular conductor placed on the right-hand side of  $Oy$  axis

This system is an element of the high current busducts as presented in figure 2 [3].

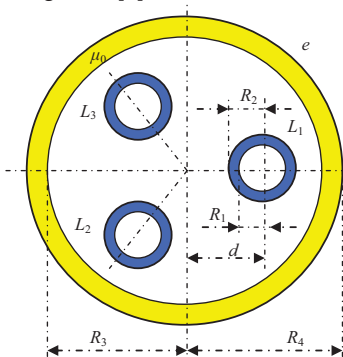


Fig. 2. Three-pole three-phase high current transmission line

In this paper we are going to show you how the magnetic field looks when the conductor axis – screen axis distance changes.

## The magnetic field generated by the current flowing in an internal parallel tubular conductor

Let us consider a magnetic field in the shield of conductivity  $\gamma_2$ , with internal radius  $R_3$  and external radius  $R_4$ , parallel to a non-coaxial internal tubular conductor with conductivity  $\gamma_1$ , internal radius  $R_1$  and external radius  $R_2$  with complex rms current  $I_1$ . The distance between the axes of the conductors is  $d$  (fig. 1). This current generates sinusoidal alternating magnetic field  $\underline{H}^w(r_{XY})$ , which can be expressed in local cylindrical coordinates  $(r, \Theta)$  of the shield.

The vector magnetic potential created by the current  $I_1$  has one component only along the  $Oz$  axis and is a potential created by the source external to the second conductor i.e.

$$(1) \quad \underline{A}^w(r_{XY}) = \mathbf{1}_z \underline{A}^w(r_{XY})$$

and according to its definition, in the system of  $(\rho, \Phi, z)$  cylindrical coordinates connected with the second conductor we have

$$(2) \quad \text{rot} \underline{A}^w(r_{XY}) = \mu_0 \underline{H}^w(r_{XY})$$

where the magnetic field

$$(3) \quad \underline{H}^w(r_{XY}) = \mathbf{1}_\Phi \frac{I_1}{2\pi r_{XY}} = \mathbf{1}_\Phi \underline{H}^w(r_{XY})$$

From these formulas we obtain the equation [4]

$$(4) \quad -\frac{d\underline{A}^w(r_{XY})}{dr_{XY}} = \mu_0 \frac{I_1}{2\pi r_{XY}}$$

hence

$$(5) \quad \underline{A}^w(r_{XY}) = \frac{\mu_0 I_1}{2\pi} \ln \frac{1}{r_{XY}} + \underline{A}_0$$

where the  $\underline{A}_0$  constant can be adopted freely.

The above vector magnetic potential can be expressed by the local cylindrical coordinate system  $(r, \theta, z)$ , i.e.

$$\underline{A}^w(r, \theta) = \mathbf{1}_z \underline{A}^w(r, \theta), \text{ because}$$

$$(6) \quad r_{XY}^2 = r^2 + d^2 - 2rd \cos \theta$$

and then

$$(7) \quad \underline{A}^w(r_{XY}) = \underline{A}^w(r, \theta) = \frac{\mu_0 I_1}{2\pi} \ln \frac{1}{\sqrt{r^2 + d^2 - 2rd \cos \theta}} + \underline{A}_0$$

From the equation (6) we have

$$(8) \quad \frac{r_{XY}^2}{r^2} = 1 + \left(\frac{d}{r}\right)^2 - 2 \frac{d}{r} \cos \theta$$

and hence

$$(8a) \quad \ln \frac{r_{XY}}{r} = \frac{1}{2} \ln \left[ 1 + \left( \frac{d}{r} \right)^2 - 2 \frac{d}{r} \cos \theta \right]$$

and in the points for which  $r > d$ , in the expansion of the right hand side of the equation (8a) in the Fourier series<sup>1</sup> for  $n \in N$ , we have that

$$(8b) \quad \ln \frac{r_{XY}}{r} = - \sum_{n=1}^{\infty} \frac{1}{n} \left( \frac{d}{r} \right)^n \cos n\theta$$

Then

$$(8c) \quad \ln \frac{1}{r_{XY}} = \ln \frac{1}{r} + \sum_{n=1}^{\infty} \frac{1}{n} \left( \frac{d}{r} \right)^n \cos n\theta$$

Finally the vector magnetic potential in the  $X(r, \theta)$  point, for which  $r > d$ , is

$$(9) \quad \underline{A}^w(r, \theta) = \frac{\mu_0 I_1}{2\pi} \left[ \ln \frac{1}{r} + \sum_{n=1}^{\infty} \frac{1}{n} \left( \frac{d}{r} \right)^n \cos n\theta \right] + \underline{A}_0$$

The vector of the magnetic field intensity can be determined from the definition of the vectorial magnetic potential [5]

$$(10) \quad \underline{H}^w(r, \theta) = \frac{1}{\mu_0} \mathbf{rot} \underline{A}^w(r, \theta) = \mathbf{1}_r H_r^w(r, \theta) + \mathbf{1}_\theta H_\theta^w(r, \theta)$$

where

$$(10a) \quad \begin{aligned} H_r^w(r, \theta) &= - \frac{I_1}{2\pi r} \sum_{n=1}^{\infty} \left( \frac{d}{r} \right)^n \sin n\theta = \\ &= - \frac{I_1}{2\pi r} \sum_{n=0}^{\infty} \left( \frac{d}{r} \right)^n \sin n\theta \end{aligned}$$

and

<sup>1</sup> The equation [6]:  $\ln(1+x^2 - 2x \cos \theta) = -2 \sum_{n=1}^{\infty} \frac{1}{n} x^n \cos n\theta$  has been used.

$$(10b) \quad \begin{aligned} H_\theta^w(r, \theta) &= \frac{I_1}{2\pi r} \left[ 1 + \sum_{n=1}^{\infty} \left( \frac{d}{r} \right)^n \cos n\theta \right] = \\ &= \frac{I_1}{2\pi r} \sum_{n=0}^{\infty} \left( \frac{d}{r} \right)^n \cos n\theta \end{aligned}$$

The  $\underline{H}^w$  magnetic field is the field generated by a source external to the shield, so it is present both inside the screen and in its external area.

If the distance  $d = 0$ , then we have the coaxial, concentric system of two tubular conductors – fig. 3. This case is equivalent to the limitation of the (10a) and (10b) series to their zero terms only, that is for  $n=0$ . In this case the radial component of the magnetic field is  $H_r^w(r, \theta) = 0$ , and the tangent component  $H_\theta^w(r, \theta)$  is determined by the formula [7]

$$(11) \quad H_\theta^w(r, \theta) = \frac{I_1}{2\pi r}$$

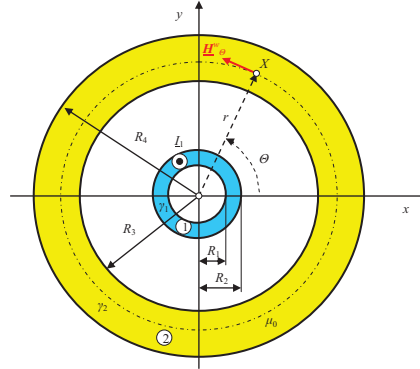


Fig. 3. Tubular screen with internal coaxial tubular conductor

#### The influence of the distance between the conductor and screen upon the magnetic field

If we introduce a relative distance between the conductor and screen

$$(12) \quad \lambda = \frac{d}{R_3} \quad (0 \leq \lambda < 1)$$

relative variable

$$(13) \quad \xi = \frac{r}{R_4}$$

and parameter

$$(14) \quad \beta = \frac{R_3}{R_4} \quad \text{where } (0 \leq \beta \leq 1)$$

and refer the magnetic field (10) to

$$(15) \quad H_0 = \frac{I_1}{2\pi R_4}$$

then we receive the relative value of the magnetic field

$$(16) \quad h_r^w(\xi, \theta) = - \frac{1}{\xi} \sum_{n=1}^{\infty} \left( \frac{\beta}{\xi} \lambda \right)^n \sin n\theta = - \sum_{n=0}^{\infty} \frac{(\beta\lambda)^n}{\xi^{n+1}} \sin n\theta$$

and

$$(16a) \quad h_\theta^w(\xi, \Theta) = \frac{1}{\xi} \left[ 1 + \sum_{n=1}^{\infty} \left( \frac{\beta}{\xi} \lambda \right)^n \cos n\Theta \right] = \sum_{n=0}^{\infty} \frac{(\beta\lambda)^n}{\xi^{n+1}} \cos n\Theta$$

The distribution of the module of this field

$$(17) \quad h^w(\xi, \Theta) = \sqrt{[h_r^w(\xi, \Theta)]^2 + [h_\theta^w(\xi, \Theta)]^2}$$

as the function of the  $\Theta$  angle, for various  $\lambda$  parameter values is presented in figure 4.

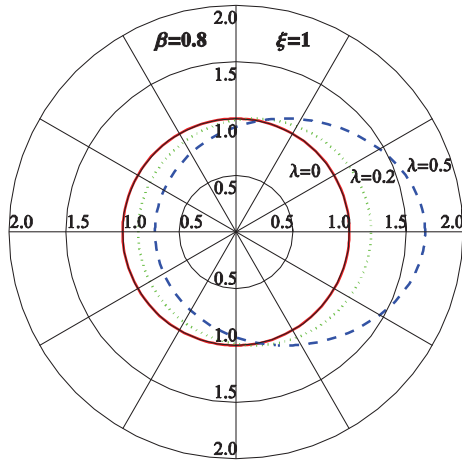


Fig. 4. The distribution of the relative value of the module of the magnetic field on the external surface of the screen generated by current in a non-coaxial internal tubular conductor placed on the right hand side of the screen axis

Therefore, the distribution of the magnetic field on the external surface is dependable on the  $\lambda$  and is a non-uniform distribution for the sake of the  $\Theta$  angle.

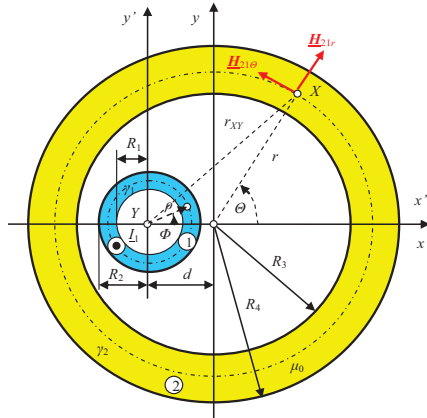


Fig. 5. Tubular screen with the internal non-coaxial tubular conductor placed on the left-hand side of the  $Oy$  axis

If the tubular conductor is on the left hand side of the screen axis (fig. 5), then we can prove, that the components of the magnetic field generated by the current flowing in this conductor in the cylindrical local coordinate system of the screen can be expressed as

$$(18) \quad \underline{H}_r^w(r, \Theta) = -\frac{I_1}{2\pi r} \sum_{n=1}^{\infty} (-1)^n \left( \frac{d}{r} \right)^n \sin n\Theta = \\ = -\frac{I_1}{2\pi r} \sum_{n=0}^{\infty} (-1)^n \left( \frac{d}{r} \right)^n \sin n\Theta$$

and

$$(18a) \quad \underline{H}_\theta^w(r, \Theta) = \frac{I_1}{2\pi r} \left[ 1 + \sum_{n=1}^{\infty} (-1)^n \left( \frac{d}{r} \right)^n \cos n\Theta \right] = \\ = \frac{I_1}{2\pi r} \sum_{n=0}^{\infty} (-1)^n \left( \frac{d}{r} \right)^n \cos n\Theta$$

Then the relative values of these components can be presented as

$$(19) \quad \underline{h}_r^w(\xi, \Theta) = -\frac{1}{\xi} \sum_{n=1}^{\infty} (-1)^n \left( \frac{\beta}{\xi} \lambda \right)^n \sin n\Theta = \\ = -\frac{1}{\xi} \sum_{n=0}^{\infty} (-1)^n \left( \frac{\beta}{\xi} \lambda \right)^n \sin n\Theta$$

and

$$(19a) \quad \underline{h}_\theta^w(\xi, \Theta) = \frac{1}{\xi} \left[ 1 + \sum_{n=1}^{\infty} (-1)^n \left( \frac{\beta}{\xi} \lambda \right)^n \cos n\Theta \right] = \\ = \frac{1}{\xi} \sum_{n=0}^{\infty} (-1)^n \left( \frac{\beta}{\xi} \lambda \right)^n \cos n\Theta$$

Then, the distribution of the module of this field as the function of the  $\Theta$  angle for various  $\lambda$  parameter values is presented in figure 6.

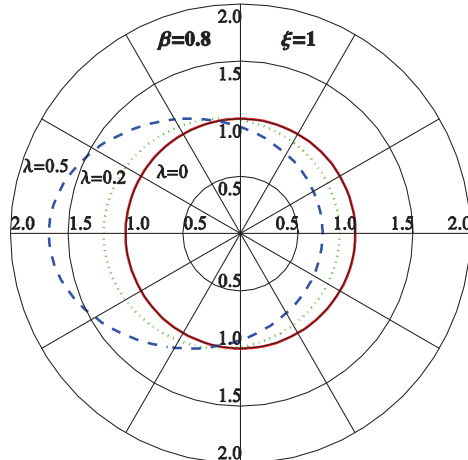


Fig. 6. The distribution of the relative value of the module of the magnetic field on the external surface of the screen generated by the current in the non-coaxial internal tubular conductor placed on the left hand side of the screen axis

In this case the magnetic field is symmetrical to the field generated by the current flowing in the conductor situated on the right hand side of the screen axis.

#### The magnetic field with the consideration of eddy currents in the screen

The  $\underline{H}^w(r, \Theta)$  magnetic field of the  $I_1$  current in the phase conductor induces  $\underline{J}_{21}(r, \Theta) = \mathbf{1}_z \underline{J}_{21}(r, \Theta)$  eddy currents in the screen (fig. 7). This eddy currents generate in the both internal and external area an reverse reaction magnetic field  $\underline{H}^{rr1}(r, \Theta)$  and  $\underline{H}^{rr2}(r, \Theta)$  respectively [8].

The  $\underline{H}^{ext}(r, \Theta)$  magnetic field in the external area ( $r \geq R_4$ ) is

$$(20) \quad \underline{H}^{ext}(r, \Theta) = \underline{H}^w(r, \Theta) + \underline{H}^{rr2}(r, \Theta)$$

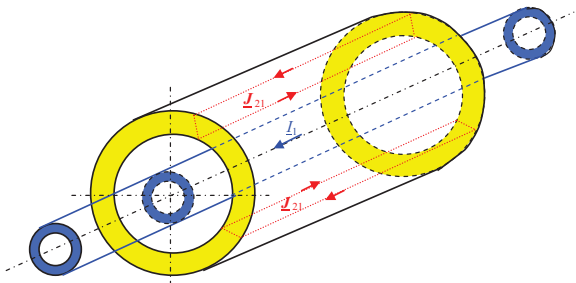


Fig.7. Eddy currents induced in the screen by the magnetic field of the own current of the phase conductor

The components of this field can be determined after solving Laplace'a and Helmholtz equations. They are given by certain combinations of modified Bessel functions. In relative values they assume the form

$$(21) \quad h_r^{ext}(\xi, \Theta) = -\sum_{n=1}^{\infty} \frac{1}{\beta} \frac{s_n}{d_n} \frac{\lambda^n}{\xi^{n+1}} \sin n\Theta$$

and

$$(21a) \quad h_{\Theta}^{ext}(\xi, \Theta) = \frac{1}{\xi} + \sum_{n=1}^{\infty} \frac{1}{\beta} \frac{s_n}{d_n} \frac{\lambda^n}{\xi^{n+1}} \cos n\Theta$$

where  $0 \leq \xi \leq \beta$  and  $0 \leq \Theta \leq 2\pi$ . In the above formulas

$$(21b) \quad s_n = I_{n-1}(\sqrt{2j}\alpha) K_{n+1}(\sqrt{2j}\alpha) - I_{n+1}(\sqrt{2j}\alpha) K_{n-1}(\sqrt{2j}\alpha)$$

and

$$(21c) \quad d_n = I_{n-1}(\sqrt{2j}\alpha) K_{n+1}(\sqrt{2j}\alpha\beta) - I_{n+1}(\sqrt{2j}\alpha\beta) K_{n-1}(\sqrt{2j}\alpha)$$

where  $\alpha = k_2 R_4$  for  $k_2 = \sqrt{\frac{\omega \mu \gamma_2}{2}} = \frac{1}{\delta_2}$ .

The relative value of the total field in the external area of the screen can be expressed as

$$(22) \quad h^{ext}(\xi, \Theta) = h_1(\xi, \Theta) + h_2(\xi, \Theta)$$

where

$$(22a) \quad h_1(\xi, \Theta) = \frac{1}{2} |h_r^{ext}(\xi, \Theta) + j h_{\Theta}^{ext}(\xi, \Theta)|$$

and

$$(22b) \quad h_2(\xi, \Theta) = \frac{1}{2} |h_r^{ext*}(\xi, \Theta) + j h_{\Theta}^{ext*}(\xi, \Theta)|$$

The distribution of this value of the external surface of the screen for various  $\lambda$  parameter values versus the  $\Theta$  angle will be presented in figure 8.

If the phase conductor is situated on the left hand side of the screen axis, then the relative components of the magnetic field for  $r \geq R_4$  ( $\xi \geq 1$ ) can be expressed as

$$(23) \quad h_r^{zew}(\xi, \Theta) = -\sum_{n=0}^{\infty} (-1)^n \frac{1}{\beta} \frac{s_n}{d_n} \frac{\lambda^n}{\xi^{n+1}} \sin n\Theta$$

and

$$(23a) \quad h_{\Theta}^{zew}(\xi, \Theta) = \frac{1}{\xi} + \sum_{n=1}^{\infty} (-1)^n \frac{1}{\beta} \frac{s_n}{d_n} \frac{\lambda^n}{\xi^{n+1}} \cos n\Theta$$

The distribution of the field module is then symmetrical to the distribution presented below.

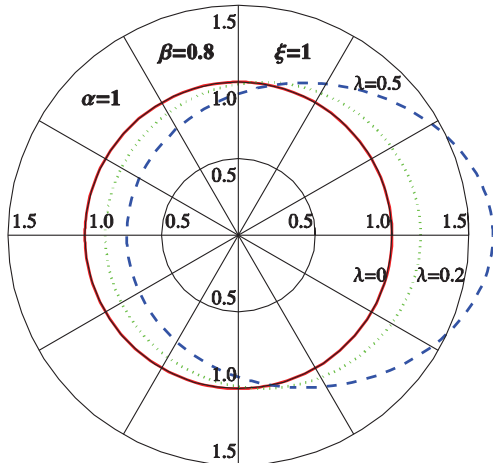


Fig. 8. The distribution of the relative module value of the total magnetic field in the external area of the screen - the phase conductor placed on the right hand side of the screen axis

### Conclusions

The presented magnetic field distribution patterns show that with the increase of the  $d$  distance between the axes of the conductors (fig. 4 and 6), the magnetic field becomes more and more irregular. So irregular will be also the values of the density of eddy currents induced in the screen as a result of the internal proximity effect. This in turn causes an irregular reverse reaction magnetic field and consequently, the total magnetic field in the screen and its surroundings is irregular (fig. 8). The analysis of the obtained formulas and numerical calculations shows also that the distribution of the magnetic field is the more irregular the higher  $\lambda$  relative distance between the conductor axis and the screen one is. Therefore, the mutual geometrical configuration of the conductor and screen has a strong effect on the magnetic field in high-current busduct.

### REFERENCES

- [1] Nawrowski R.: High-current air or SF<sub>6</sub> insulated busducts (in Polish), Wyd. Pol. Poznańska, Poznań 1998
- [2] Piątek Z.: Modeling of lines, cables and high-current busducts (in Polish), Wyd. Pol. Częst., Częstochowa 2007
- [3] Piątek Z.: Impedances of Tubular High Current Busducts. Series *Progress in High-Voltage technique*, Vol. 28, Polish Academy of Sciences, Committee of Electrical Engineering, Wyd. Pol. Częst., Częstochowa 2008
- [4] Piątek Z.: Eddy Currents Induced in the Screen of a Non-Coaxial Cable, *Przegląd Elektrotechniczny - Konferencje*, ISSN 1731-6106, R. 5, Nr 2/2007, pp. 29-32
- [5] Piątek Z., Jabłoński P.: Foundations theory of electromagnetic fields, WNT, Warsaw 2010
- [6] Mc Lachlan N.W.: Bessel functions for engineers (in Polish), PWN, Warsaw 1964
- [7] Kusiak D.: Magnetic field of two- and three-pole high current busducts, Dissertation doctor (in Polish), Pol. Częst., Wydz. Elektryczny, Częstochowa 2008
- [8] Piątek Z., Kusiak D., Szczegielniak T.: Magnetic field in three-phase symmetrical high current busduct (in Polish), Zesz. Nauk. Pol. Śl. 2009, *Elektryka*, z.1(209), pp. 37-50

**Authors:** Prof. Ph.D., Eng. Zygmunt Piątek, Institute of Environmental Engineering, ul. Brzeźnicka 60a, 42-200 Częstochowa, E-mail: [zygmunt.piatek@interia.pl](mailto:zygmunt.piatek@interia.pl)  
Ph.D., Eng. Dariusz Kusiak, Institute of Industrial Electrotechnics, Aleja Armii Krajowej 17, 42-200 Częstochowa,  
E-mail: [dariuszkusiak@wp.pl](mailto:dariuszkusiak@wp.pl)  
M.Sc., Eng. Tomasz Szczegielniak, Doctorate Study, ul. Dąbrowskiego 73, 42-200 Częstochowa,  
E-mail: [szczegielniak@interia.pl](mailto:szczegielniak@interia.pl)